Dynamics near a heteroclinic network

2005 Nonlinearity 18 391

(http://iopscience.iop.org/0951-7715/18/1/019)

INSTITUTE OF PHYSICS PUBLISHING NONLINEARITY

Nonlinearity **18** (2005) 391–414 doi:10.1088/0951-7715/18/1/019

Dynamics near a heteroclinic network

Manuela A D Aguiar[1,2], **Sofia B S D Castro**[1,2] **and Isabel S Labouriau**[1]

[1] Centro de Matemática da Universidade do Porto[3], Rua do Campo Alegre 687, 4169-007 Porto, Portugal
[2]Faculdade de Economia, Universidade do Porto, Rua Dr. Roberto Frias, 4200-464 Porto, Portugal

E-mail: maguiar@fep.up.pt, sdcastro@fep.up.pt and islabour@fc.up.pt

Received 20 January 2004, in final form 24 September 2004
Published 25 October 2004
Online at stacks.iop.org/Non/18/391

Recommended by M J Field

Abstract

We study the dynamical behaviour of a smooth vector field on a three-manifold near a heteroclinic network. Under some generic assumptions on the network, we prove that every path on the network is followed by a neighbouring trajectory of the vector field—there is switching on the network. We also show that near the network there is an infinite number of hyperbolic suspended horseshoes. This leads to the existence of a horseshoe of suspended horseshoes with the shape of the network.

Our results are motivated by an example constructed by Field (1996 *Lectures on Bifurcations, Dynamics, and Symmetry* (*Pitman Research Notes in Mathematics Series* vol 356) (Harlow: Longman)), where we have observed, numerically, the existence of such a network.

Mathematics Subject Classification: 37C10, 37C29, 37C80, 37D45, 37C50, 34F05

M This article features online multimedia enhancements

1. Introduction

Heteroclinic phenomena, such as cycles and networks, have attracted the attention of many authors in the last 25 years. It has been observed that these phenomena are often associated with complex dynamics. Although there are many results on the dynamics arising from the existence of heteroclinic cycles, there are still very few analytic results concerning the

[3] CMUP is supported by Fundação para a Ciência e a Tecnologia through Programa Operacional Ciência, Tecnologia e Inovação (POCTI) and Programa Operacional Sociedade da Informação (POSI) of Quadro Comunitário de Apoio III (2000–2006) with European Union funding (FEDER) and national funding.

dynamic behaviour induced by a network in its vicinity. These are the main concerns of this paper.

We shall think of a *heteroclinic cycle* as a cycle of (relative) equilibria connected by non-trivial intersections of their invariant manifolds. In this case we say there is a *connection* between the equilibria. Nearby trajectories may follow along the connections.

In some examples there is more than one heteroclinic cycle for the same dynamical system. When coexisting heteroclinic cycles have a nonempty intersection we talk about a *heteroclinic network*.

In the networks we consider some connections that arise through transverse intersections of invariant manifolds, while the other connections are induced by symmetry.

If there are trajectories along all the sequences of connections in the network, we say there is *switching* on the network.

We prove switching under generic assumptions on a network. Switching arises through the transverse intersections and the existence of complex eigenvalues. Our approach also shows the existence of a horseshoe of suspended horseshoes with the shape of the network. Suspended horseshoes are a consequence of the complex eigenvalues at the nodes of the network, as in the Shilnikov bifurcation.

There have been examples of robust heteroclinic cycles involving periodic trajectories as well as equilibria, using various symmetry groups and settings. Symmetry is a natural setting for the existence of persistent heteroclinic cycles since, as shown by Field [12] in 1980, symmetry can force non-transversal intersections of invariant manifolds. If the connections between the (relative) equilibria in the cycle are contained in fixed-point spaces, the invariance of these spaces plus the robustness of the connections inside the spaces guarantees robustness of the cycle. A review of the results on robust heteroclinic cycles up to 1997 can be found in Krupa [22]. For more recent developments, see Chossat *et al* [10], Ashwin and Chossat [5], Field and Swift [15] and Dias *et al* [11].

The phenomenon of bifurcation from heteroclinic cycles has been studied by Campbell and Holmes [8] and Worfolk [29]. In the work of Worfolk, complicated dynamics appears in the neighbourhood of a perturbed heteroclinic cycle due to the existence of Smale horseshoes embedded in the flow. A review of results on the dynamical consequences of some homoclinic and heteroclinic motions in three and four dimensions is described by Wiggins [28].

Early examples of heteroclinic networks may be found in Melbourne *et al* [24], Silber *et al* [27], Lauterbach and Roberts [23], Field and Richardson [14], Ashwin and Field [6] and Kirk and Silber [21].

Kirk and Silber raise two questions. The first concerns the stability of the heteroclinic cycles that form the network. This issue is also addressed by Brannath [7], who provides the necessary and sufficient conditions for heteroclinic cycles to be *relatively* asymptotically stable—given that being part of a network prevents them from being asymptotically stable attractors. The second question concerns the dynamics associated with the existence of the heteroclinic network. They conjecture the existence of random switching between the cycles of the network in case the 'dynamics along the network include sequences of visits to the equilibria more complicated than those associated with a simple heteroclinic cycle'. We prove this conjecture for certain heteroclinic networks.

An example of switching appears in Guckenheimer and Worfolk [19]. In 2003, the phenomenon of switching was introduced by Armbruster *et al* [4] as noise-induced. We show the existence of switching without noise.

Numerical evidence of complex behaviour near a network was observed by, for example, Field [16] and Chawanya [9]. An analytic approach appears in Reissner [25] using the

context of time-reversible systems, partly for simplifying the analysis. We address the problem analytically without the use of reversing-symmetries.

In appendix A of [16], Field conjectures that a given dynamical system in $\mathbf{R}^4$ possesses a network of heteroclinic cycles leading to horseshoe dynamics. These conjectures and further discussions with Field motivated our study of the dynamical system that we present here. We show Field's conjectures to be true for a class of vector fields with a network of the same type. In particular, we prove Field's conjectures concerning the dynamics and the existence of switching for his example, assuming the existence of numerically observed connections. Our results hold under general assumptions (examples are given in Aguiar *et al* [2]) and are therefore not strictly about Field's example.

We conclude this introduction with a description of our results and their presentation.

Framework of the paper

In the next section we present and discuss some definitions which will be used throughout this paper. The following section contains the description of the dynamical system in appendix A of Field [16] and its symmetries. Numerical evidence of the connections and the way symmetry can be used to generate the network are described in sections 4 and 5, respectively. The connections between saddles are obtained by numerical integration of the dynamical system (details in our appendix). We then use the symmetry of the system to show how all observed connections can be obtained using the group action on a selected set of numerically observed connections. In section 5, we also use symmetry to reduce the original network to a quotient network with two nodes which will be used in subsequent sections.

Section 6 is a study of the dynamics in a neighbourhood of a network with two nodes. The results are general and do not depend on the first sections, but they apply to the quotient network of subsection 5.1. This section starts with a technical description of the geometry of the Poincaré map near the connections. This is then used to establish switching and dynamics-related results. We prove the existence of horseshoe dynamics in a neighbourhood of heteroclinic cycles in the two-node network: switching both at every node of the network and switching on the network. The existence of switching on the network amounts to proving that all the connections of the network are realized by nearby dynamics. These proofs rely on some general hypotheses on the dynamical system (which are satisfied by generic systems besides the one studied in [16]). We make a couple of more restrictive hypotheses to simplify calculations and include some resonances present in this particular dynamical system. The resonance-related hypotheses are not essential for the proof, which holds without them although with dirtier calculations.

The results are presented in four subsections. In the first subsection, we show the existence of switching at every node of the two-node network. In the following two subsections, we prove the existence of suspended horseshoe dynamics in the neighbourhood of heteroclinic cycles of the two-node network, with all the usual consequences for the dynamics. In actual fact, we prove that there exist an infinite number of hyperbolic suspended horseshoes. Subsection 6.3 has a proof of the hyperbolicity of the Poincaré map. This guarantees that invariant sets persist under symmetry-breaking perturbations. Hence, the horseshoes and switching persist generically. Switching on the network is proved in subsection 6.4.

Section 7 is devoted to showing how results obtained for the quotient network translate to the original setting. We show that the switching obtained in the quotient network can be lifted to the original network, thus proving that all the connections of the original network are realized by the dynamics.

2. Preliminaries

Let X be a smooth vector field on $\mathbf{R}^m$.

Suppose that A is a compact invariant set for the flow of X. Following [16], we say that A is an *invariant saddle* if both $\overline{W^s(A)\backslash A}$ and $\overline{W^u(A)\backslash A}$ contain A. Note that invariant saddles do not have to be hyperbolic, although in our example they are.

We say saddles A_1 and A_2 are a *pair of connected saddles* if there exists a connection from A_1 to A_2. A *connection* from saddle A_1 to saddle A_2 (denoted $[A_1 \to A_2]$) is any one of the trajectories contained in $W^u(A_1) \cap W^s(A_2)$.

Let $\{A_i, i = 0, \ldots, n-1\}$ be a finite ordered set of mutually disjoint invariant saddles for the vector field X. If there are connections $[A_i \to A_{i+1}]$ for $i = 0, \ldots, n-1 \pmod n$, then we say that

$$\bigcup_{i=0}^{n-1} A_i \cup [A_i \to A_{i+1}],$$

is a *heteroclinic cycle* with invariant saddles $\{A_i\}$.

We think of a *heteroclinic network*, usually denoted by Σ, as a finite union of heteroclinic cycles. The saddles defining the heteroclinic cycles and network are called *nodes* of the network and we denote them by n_i. We define a *subnetwork* as a network consisting of the union of fewer cycles, not necessarily involving smaller number of nodes. We shall assume that the network is connected. The disconnected case is a disjoint union of connected networks.

This is a loose definition. In the literature, several definitions have appeared, mostly due to the different needs of the issues addressed. See Field and Richardson [14], Field [16], Kirk and Silber [21] and Dias *et al* [11], where the expressions *web*, *complex* and *network* are used for roughly the same concept.

Ashwin and Field present in [6] a definition of a heteroclinic network that generalizes the definitions of a heteroclinic network thus far, and introduces the concept of depth in the network. They define a heteroclinic network as a flow-invariant set that is indecomposable but not recurrent.

Their definition covers many previously discussed examples of heteroclinic behaviour but not the Shilnikov network of Field's example in appendix A of [16] that we study here as we establish the existence of an infinite set of recurrent points in the neighbourhood of the network.

Let Σ be a network with a finite set of nodes. We define a *path* on Σ as a bi-infinite sequence $(c_j)_{j\in\mathbf{Z}}$ of connections in Σ such that $c_j = [n_{j-1} \to n_j]$, with n_j nodes of Σ.

We say there is *switching at a node n* if, for any neighbourhood of a point in a connection leading to node n, trajectories starting in that neighbourhood will follow along all the possible connections forward from n.

Let N_Σ be any neighbourhood of a network Σ and U_n arbitrary neighbourhoods of the nodes $n \in \Sigma$. For every connection contained in Σ, let p be an arbitrary point on it and consider an arbitrary neighbourhood U_p of each p. We say there is *switching on the network* if, for each path $(c_i)_{i\in\mathbf{Z}}$ contained in Σ, there is a trajectory $x(t) \subset N_\Sigma$ and sequences (t_i), (s_i) with $t_{i-1} < s_i < t_i$ such that $x(s_i) \in U_{p_i}$ and $x(t_i) \in U_{n_i}$, where $p_i \in c_i$.

We remark that switching at every node is not enough to guarantee the existence of switching on the network. In fact, the latter is a much stronger concept.

Some of the results of this paper can be rephrased in terms of shadowing (see section 5.3 of [17], chapter 1, section 3 and chapter 2, section 3 of [3] for details and definitions). Two connections $[M_{-1} \to N], [N \to M_{+1}]$ at the same node N of a network Σ can be seen as

a pseudo-orbit of X, by removing the parts of the connections that lie near N. Switching at N means that these pseudo-orbits can be shadowed.

A path on Σ can also be seen as a pseudo-orbit of X, with infinitely many discontinuities. Switching on Σ means that these infinite pseudo-orbits can also be shadowed.

3. Equations and symmetries

Consider the family of differential equations in $\mathbf{R}^4$, given by:

$$\begin{aligned}
\dot{x}_1 &= \lambda x_1 - |x|^2 x_1 + \beta(x_1^2 x_2 - y_1^2 x_2 - 2x_1 y_1 y_2) + \gamma(x_2^3 - 3x_2 y_2^2),\\
\dot{y}_1 &= \lambda y_1 - |x|^2 y_1 + \beta(-x_1^2 y_2 + y_1^2 y_2 - 2x_1 y_1 x_2) + \gamma(-y_2^3 + 3x_2^2 y_2),\\
\dot{x}_2 &= \lambda x_2 - |x|^2 x_2 + \beta(x_1 x_2^2 - x_1 y_2^2 + 2y_1 x_2 y_2) + \gamma(x_1^3 - 3x_1 y_1^2),\\
\dot{y}_2 &= \lambda y_2 - |x|^2 y_2 + \beta(y_1 x_2^2 - y_1 y_2^2 - 2x_1 x_2 y_2) + \gamma(y_1^3 - 3x_1^2 y_1)
\end{aligned} \tag{1}$$

with $x = (x_1, y_1, x_2, y_2)$ and real parameters λ, β and γ. These equations are studied by Field [16] as a counterexample to the maximal isotropy subgroup conjecture. We describe some of its properties and refer the reader to appendix A of [16] for more details.

Identifying $\mathbf{R}^4 \approx \mathbf{C}^2$, we may rewrite the equations in complex coordinates (z_1, z_2), where $z_j = x_j + iy_j$, $j = 1, 2$. With this notation, the family (1) is equivariant by the discrete group Γ of order 40 generated by

$$\begin{aligned}
s(z_1, z_2) &= (\omega z_1, \omega^2 z_2), && \text{of order 5,}\\
t(z_1, z_2) &= (\overline{z}_2, z_1), && \text{of order 4,}\\
-I(z_1, z_2) &= (-z_1, -z_2), &&
\end{aligned} \tag{2}$$

where $\omega = \mathrm{e}^{2\pi \mathrm{i}/5}$. We denote by $\mathbf{Z}_n(g)$ the subgroup of order n generated by an element $g \in \Gamma$. There are five copies of each of the following proper fixed-point spaces ([16], lemma A.7):

$$L_1 = \mathrm{Fix}(\mathbf{Z}_4(t)) = \{(x_1, 0, x_1, 0) : x_1 \in \mathbf{R}\},$$

$$L_2 = \mathrm{Fix}(\mathbf{Z}_4(-t)) = \{(x_1, 0, -x_1, 0) : x_1 \in \mathbf{R}\},$$

$$P_1 = \mathrm{Fix}(\mathbf{Z}_2(t^2)) = \{(x_1, 0, x_2, 0) : x_1, x_2 \in \mathbf{R}\},$$

$$P_2 = \mathrm{Fix}(\mathbf{Z}_2(-t^2)) = \{(0, y_1, 0, y_2) : y_1, y_2 \in \mathbf{R}\}.$$

From now on we fix parameter values as follows:

$$\lambda > 0, \qquad \gamma < 0, \qquad \beta > 0, \qquad \gamma + 3\beta > 0 \qquad \text{and} \qquad |\beta + \gamma| < 2. \tag{3}$$

For these parameter values the cubic term of (1) is contracting (lemma A.10 of [16]). By the invariant sphere theorem ([13, 16]), the dynamics of (1) can be reduced to an invariant three-dimensional sphere that is globally attracting, in the sense that every trajectory except the trivial equilibrium is forward asymptotic to the sphere. The invariant sphere can be obtained as the graph of a function from the unit sphere in $\mathbf{R}^4$ into $\mathbf{R}^+$. In the particular case $\beta = -\gamma$, this function is constant and thus the topological sphere is indeed the geometric sphere of radius $\sqrt{\lambda}$. We restrict our attention to the flow on the topological sphere, denoted S^3.

The following results on the dynamics on the fixed-point spaces are relevant for later sections.

- Each of the axes L_1 and L_2 meets S^3 at two equilibria, $\pm a(\lambda)$ and $\pm b(\lambda)$, respectively. These are the only non-trivial equilibria on P_1 ([16], lemma A.11) (see figure 1(*a*)).

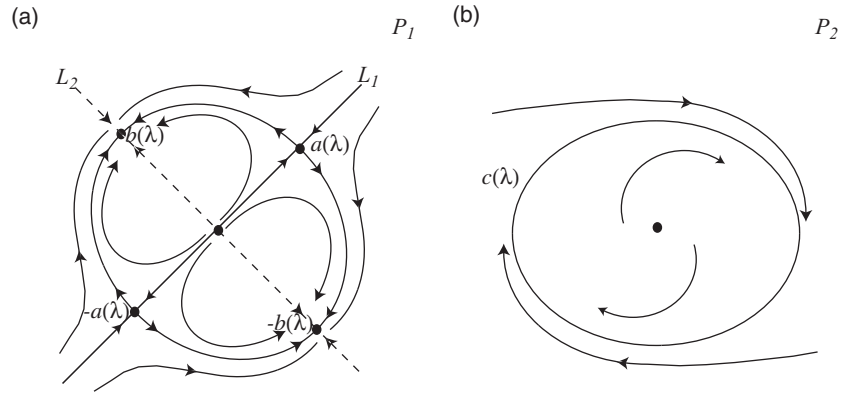

Figure 1. Dynamics of Field's example on the fixed-point planes.

- For the flow restricted to P_1, the points $\pm b(\lambda)$ are sinks, $\pm a(\lambda)$ are saddles ([16], lemma A.14) (see figure 1(*a*)).
- The intersection of S^3 with the plane P_1 consists of four arcs formed by trajectories joining $\pm a(\lambda)$ to $\pm b(\lambda)$ (see figure 1(*a*)).
- In the restriction to S^3, $\dim(W^u(b(\lambda))) = 2$ and $\dim(W^s(a(\lambda))) = 2$ and both $W^u(b(\lambda))$ and $W^s(a(\lambda))$ are transverse to the plane P_1 ([16], lemma A.14).
- There are no non-trivial equilibria on the plane P_2 ([16], proposition A.15). The intersection of P_2 and S^3 is a periodic trajectory, $c(\lambda)$, that attracts all points in $P_2 - \{0\}$ (see figure 1(*b*)).
- The only equilibria of (1) are the origin, $\pm s^n a(\lambda)$ and $\pm s^n b(\lambda)$ ($n = 0, \ldots, 4$), with s as in (2).

The dynamics in the conjugates by Γ of these fixed-point spaces is similar.

Field conjectures the existence of a heteroclinic network involving $a(\lambda)$, $b(\lambda)$ and $c(\lambda)$ and all their conjugates and that there is chaotic dynamics near the network. Numerical evidence for such a network is discussed in the following two sections. The existence of switching and chaotic dynamics near the network is left for the last sections, where results are proved for a theoretically defined network related to Field's example. Simpler examples with similar networks are constructed in [1, 2]. For these examples, Field's conjecture can be proved analytically.

4. Numerical evidence of connections

From now on we assume $\lambda = 1$ fixed and we omit references to λ in the text, using $a = a(1)$, $b = b(1)$ and $c = c(1)$. For the numerical computations we used $\beta = 1$ and $\gamma = -0.6$.

In our numerical study we used the dynamical systems package Dstool (dynamical systems toolkit) [18]. Our procedure was based on the fact that heteroclinic phenomena are related to nontransient intermittent behaviour: a trajectory in the neighbourhood of a heteroclinic cycle or network will move from one invariant saddle to the next, spending a long time near each invariant saddle.

In our Dstool specification of Field's example we incorporated a C-routine: we consider a neighbourhood of each invariant equilibrium and periodic trajectory; at each Dstool iteration, the C-routine inspects if the actual position in the phase space is within any of the neighbourhoods, and in that case it prints the identification of the corresponding equilibrium

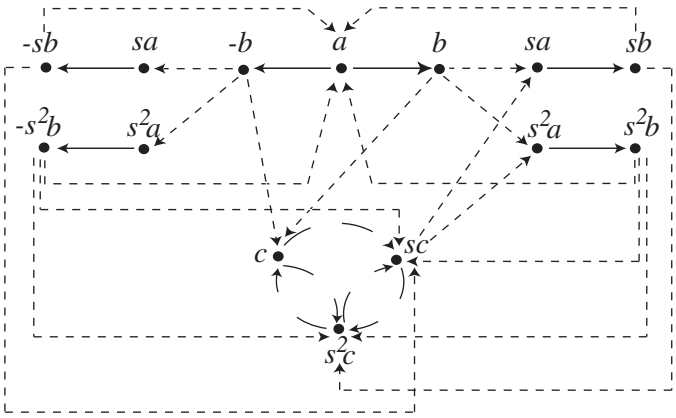

Figure 2. Schematic representation of a subnetwork. Solid lines indicate connections found analytically inside fixed-point subspaces and dashed lines indicate transversal connections found numerically. Symmetry applied to this subnetwork produces the full network.

or periodic trajectory and the distance in each coordinate between the actual position and that of the invariant saddle.

The appendix contains a more detailed explanation of how the C-routine works.

The sequences produced give evidence of the existence of several connections. We single out the following:

- $[a \to b]$ (also found analytically),
- $[b \to \pm s(a)]$,
- $[b \to c]$,
- $[b \to sc]$,
- $[c \to a]$,
- $[c \to sa]$,
- $[c \to sc]$,

with s the element of Γ defined in (2).

As we show in the next section, the connections listed above, together with the symmetry of the problem, suffice to produce all the connections observed numerically as well as to construct a heteroclinic network Σ.

Note that we do not know the multiplicity of these connections. This seems to be impossible to determine numerically.

The periodic trajectory c on the plane P_2 is a hyperbolic saddle whose unstable manifold may have dimension 2 or 3. Numerical computations with global analysis of invariant objects (GAIO) (Junge [20]) indicate that the unstable manifold of the periodic trajectory is two-dimensional.

In the cases where invariant manifolds of dimension $\geqslant 2$ of two equilibria intersect, numerical computations with GAIO indicate that the intersection is transversal.

5. Symmetries and heteroclinic networks

Given a connection in (1), the symmetry can be used to obtain other connections. When applied to the connections obtained numerically, it produces a heteroclinic network (see figure 2).

Table 1. Isotropy subgroups and orbits for the saddles a, b, c of (1).

Saddle	Group orbit	Isotropy subgroup
a	$\{\pm s^n a\}$	$\mathbf{Z}_4(t)$
b	$\{\pm s^n b\}$	$\mathbf{Z}_4(-t)$
c	$\{s^n c\}$	$\mathbf{Z}_2(-I) \times \mathbf{Z}_4(t)$

Table 2. New connections between pairs of connected saddles generated by symmetry.

Original connection	New connections	Conditions	Total number of different connections
$[a \to b]$	$\pm s^n[a \to \pm b]$	$n \in \mathbf{Z}_5$	20
$[b \to \pm sa]$	$\pm s^k[b \to \pm s^n a]$	$k, n \in \mathbf{Z}_5, n \neq 0$	80
$[b \to c]$	$s^n[\pm b \to c]$	$n \in \mathbf{Z}_5$	10
$[b \to sc]$	$s^k[\pm b \to s^n c]$	$k, n \in \mathbf{Z}_5, n \neq 0$	40
$[c \to a]$	$s^n[c \to \pm a]$	$n \in \mathbf{Z}_5$	10
$[c \to sa]$	$s^k[c \to \pm s^n a]$	$k, n \in \mathbf{Z}_5, n \neq 0$	40
$[c \to sc]$	$s^k[c \to s^n c]$	$k, n \in \mathbf{Z}_5, n \neq 0$	20

Let X be a smooth vector field on $\mathbf{R}^m$. Consider a pair of connected saddles A_1, A_2 for X. Let Γ be a discrete Lie group acting on $\mathbf{R}^m$. If X is Γ-equivariant, then for $g \in \Gamma$ we have

$$W^u(g \cdot A_1) \cap W^s(g \cdot A_2) = g \cdot (W^u(A_1) \cap W^s(A_2)).$$

Thus we have an action of Γ in the set consisting of pairs of connected saddles together with the connections between them. The group Γ acts on $\Gamma(A_1) \times \Gamma(A_2)$ by $g \cdot (A_1, A_2) = (g \cdot A_1, g \cdot A_2)$. The connections we can obtain by symmetry from $[A_1 \to A_2]$ may be identified with (A_i, A_j) in the group orbit $\Gamma((A_1, A_2))$. Let Γ_{A_i} be the isotropy subgroup of A_i. Since (A_1, A_2) has isotropy subgroup $\Gamma_{A_1} \cap \Gamma_{A_2}$, the order of the group orbit $\Gamma((A_1, A_2))$ is

$$\#\Gamma / \#(\Gamma_{A_1} \cap \Gamma_{A_2}). \tag{4}$$

For the group Γ and the saddles a, b, c of section 3 the isotropy subgroups and orbits are listed in table 1.

The 220 pairs of connected saddles listed in table 2 were obtained by computing the Γ orbits of the pairs of section 4. No other pairs of connected saddles were found numerically.

Theorem 1. *Let Γ be the finite group of section 3 and X a Γ-equivariant vector field with invariant saddles a, b and c and the original connections in the first column of table 2. Then X has a heteroclinic network Σ involving all the invariant saddles of $\Gamma(\{a, b, c\})$ and all the pairs of connected saddles in table 2.*

Proof. Since the symmetry group is finite, given the original connections, we get by symmetry a finite number of connections which are given in table 2. For each invariant saddle, there is at least one connection starting and at least one connection ending at that saddle. Thus, there are sequences of connections starting and ending at the same invariant saddle, and every connection belongs to at least one of those sequences. Each sequence of connections gives a heteroclinic cycle. The union of all the heteroclinic cycles is a heteroclinic network involving all the invariant saddles of equations (1). □

If there are more connections involving the saddles of $\Gamma(\{a, b, c\})$, then, by the same method, we obtain a larger network of which Σ (in theorem 1) is a subnetwork.

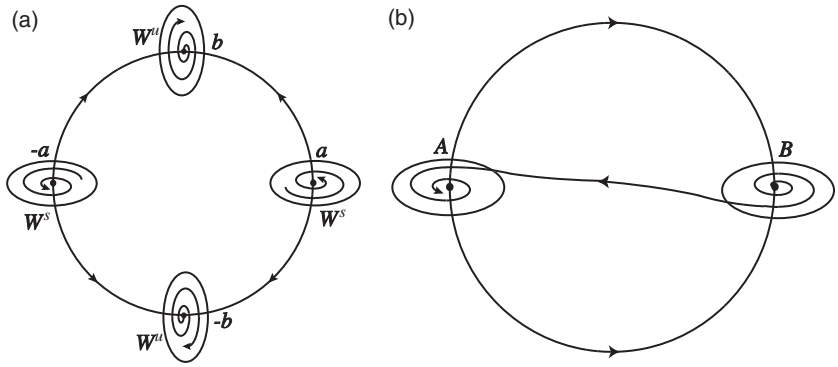

Figure 3. (*a*) Dynamics of Field's example near the plane P_1 (similar to figure 11 in [16]). (*b*) Schematic representation of the quotient subnetwork of equilibria. The line from B to A represents eight connections.

Remark. The pairs of connected saddles in $\Gamma(\{a, b, c\}) \times \Gamma(\{a, b, c\})$ that were *not* found correspond to:

- all the connections $[g_1 a \to g_2 x]$ with $x = a, c$;
- all the connections $[g_1 x \to g_2 b]$ with $x = b, c$;
- $\Gamma[a \to \pm sb]$ i.e. $\pm s^k[a \to \pm s^n b]$;
- $\Gamma([b \to a])$ i.e. $\pm s^k[b \to \pm a]$;
- $\Gamma([c \to c])$ i.e. $s^k[c \to c]$,

where g_1, g_2 are arbitrary elements of Γ, $k, n \in \mathbf{Z}$ (mod5) and $n \neq 0$.

5.1. Quotient network

Suppose there are no connections besides those of table 2 and that there is only one connection for each pair of connected saddles. A considerable simplification is obtained if we restrict our attention to the subnetwork corresponding to the conjugates of the equilibria a, b. This reduces the number of pairs of connected saddles from 220 to 100. The subnetwork of equilibria is already interesting from the point of view of the dynamics and, henceforth, we restrict our attention to this subnetwork.

A further reduction consists in identifying some of the points in a group orbit, as we proceed to describe.

The subgroup $G = \mathbf{Z}_{10}(-s) \subset \Gamma$ acts fixed point freely on $\mathbf{R}^4$ and freely on the invariant sphere S^3. We work on the orbit space S^3/G, a three-dimensional manifold. The restriction of (1) to S^3 defines a quotient vector field on S^3/G. The subgroup $H = \mathbf{Z}_4(-t) \subset \Gamma$ induces an (non-free) action on S^3/G.

The invariant circles with four equilibria in the group orbit of $S^3 \cap \mathrm{Fix}(\mathbf{Z}_2(t^2))$ by Γ drop down to an H-invariant circle with two equilibria A, B in S^3/G (see figure 3). Note that these equilibria correspond, respectively, to the group orbits $\Gamma(a)$ and $\Gamma(b)$, since $ta = a$ and $tb = -b$. The equilibria A and B are fixed by H and semicircles are interchanged by H. More importantly, the group H acts freely on the two-dimensional stable and unstable manifolds of A and B, and thus there is no loss of information in passing to the quotient.

Thus, the 20 connections in S^3 forming the G-orbit of the two connections $[a \to \pm b]$ drop down to two connections from A to B in S^3/G.

Consider one of the connections $[b \to sa]$. As we have already seen, its H-orbit has four elements. The G-orbit of these four connections consists of 40 connections in S^3 that drop down to four connections from B to A in S^3/G (given by the action of H). Yet another four connections drop down from the 40 pairs in the orbit of $[b \to -sa]$.

In conclusion, the heteroclinic network between the 20 equilibria in S^3 drops down, by the reduction to the orbit space S^3/G, to a quotient heteroclinic network between the two equilibria A and B. There are two connections from A to B and eight connections from B to A as shown in figure 3. These are representatives of all the connections in the subnetwork of equilibria.

6. The Poincaré map

In this section we describe the geometry of the flow in a neighbourhood of a network involving two equilibria A, B, like the quotient network of subsection 5.1. Examples of vector fields for which such a network can be found analytically are reported in [1, 2]. We are concerned with persistent behaviour and thus many of the calculations are illustrated for a particular case. The results hold for any network with a similar structure, and so we state the properties that are going to be used.

(H0) Let X be a smooth vector field in a three-manifold with two equilibria A, B.

Let λ_e and $\alpha_e \pm \mathrm{i}\beta_e$ be the eigenvalues of the linearization of X at $e = A, B$. We consider

(H1) $\lambda_A > 0, \quad \alpha_A < 0, \quad \beta_A > 0, \qquad \lambda_B < 0, \quad \alpha_B > 0, \quad \beta_B > 0,$

(H2) $-\alpha_A\beta_B = \beta_A\alpha_B,$

(H3) $\dfrac{\alpha_A\lambda_B}{\lambda_A\alpha_B} = 1.$

Hypotheses (H1), (H2) and (H3) are satisfied at the equilibria of (1). The results of this paper still hold if the eigenvalues do not satisfy (H2) and (H3), with slightly more complicated proofs.

A saddle with a pair of complex eigenvalues in $\mathbf{R}^3$ will not have resonances of order 1. By theorem 1 in Samovol [26], the flow is C^1 linearizable around each equilibrium. In fact, the only obstruction to C^1 linearization would come from terms of degree 2, which do not exist here.

In neighbourhoods N_e of e, $e = A, B$ we choose coordinates for which the flow is linear, with the equilibrium at the origin and such that the local stable and unstable manifolds are either the horizontal plane or the vertical axis. Using polar coordinates (r, θ) in the horizontal plane and z for the vertical axis, we have for A

$$W^u_{\mathrm{loc}}(A) = \{(0, 0, z) : z \in \mathbf{R}\},$$
$$W^s_{\mathrm{loc}}(A) = \{(r, \theta, 0) : r \in \mathbf{R}^+, \theta \in [-\pi, \pi]\},$$

and for B

$$W^s_{\mathrm{loc}}(B) = \{(0, 0, z) : z \in \mathbf{R}\},$$
$$W^u_{\mathrm{loc}}(B) = \{(r, \theta, 0) : r \in \mathbf{R}^+, \theta \in [-\pi, \pi]\}.$$

Inside each neighbourhood N_e, $e = A, B$ we consider cylindrical neighbourhoods of the equilibria (see figure 4), delimited by the surfaces

$$\mathcal{W}_e = \{(r, \theta, z) : r = r_e, \theta \in [-\pi, \pi] \text{ and } -z_e < z < z_e\},$$
$$\mathcal{T}_e = \{(r, \theta, z) : r < r_e, \theta \in [-\pi, \pi] \text{ and } z = z_e\},$$
$$\mathcal{B}_e = \{(r, \theta, z) : r < r_e, \ \theta \in [-\pi, \pi] \text{ and } z = -z_e\}.$$

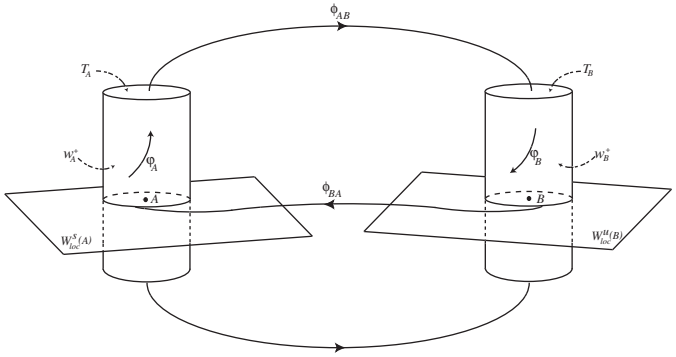

Figure 4. Transition maps φ_B, ϕ_{AB}, φ_A, ϕ_{BA}.

With this notation the network of section 5.1 corresponds to the following assumptions.

(H4) The flow connects the positive half-axis $z^+ = \{(0, 0, z) : z > 0\}$ in N_A to the positive half-axis z^+ in N_B and the negative half-axis z^- in N_A to the negative half-axis z^- in N_B. These are the only connections $[A \to B]$.

(H5) The flow from $\mathcal{T}_A$ and $\mathcal{B}_A$ follows these connections in flow-box fashion. Roughly speaking, it maps $\mathcal{T}_A$ into $\mathcal{T}_B$ and $\mathcal{B}_A$ into $\mathcal{B}_B$.

(H6) There are exactly m connections from $W^u_{\rm loc}(B)$ to $W^s_{\rm loc}(A)$, and the two-dimensional manifolds meet transversely at these connections. The flow from $\mathcal{W}_B$ to $\mathcal{W}_A$ follows these connections in flow-box fashion in suitable neighbourhoods of the connections.

In N_A and N_B, let $\mathcal{W}_{e_0}$, $e = A, B$ be given by

$$\mathcal{W}_{e_0} = \{(r, \theta, z)\ r = r_e \text{ and } z = 0\},$$

i.e. $\mathcal{W}_{A_0} = W^s_{\rm loc}(A) \cap \mathcal{W}_A$ and $\mathcal{W}_{B_0} = W^u_{\rm loc}(B) \cap \mathcal{W}_B$. Assumption (H6) means that exactly m points in the circle $\mathcal{W}_{B_0}$ are mapped by the flow into m points in $\mathcal{W}_{A_0}$.

Let $p_1, p_2 \in \mathcal{W}_{A_0}$ be two of these connection points (possibly the same) and consider neighbourhoods $p_1 \in R_1$ and $p_2 \in R_2$ in $\mathcal{W}_A$. Suppose $R_1 \cap R_2 = \emptyset$ if $p_1 \neq p_2$ and $R_1 = R_2$ if $p_1 = p_2$.

In what follows we define a Poincaré map Ψ for the points in R_1 whose image by the flow follows the connection of the positive half-axes in (H6) and then returns to R_2 along one of the connections in (H6). The Poincaré map will be the composition of transition maps (see figure 4) $\Psi = \phi_{BA} \circ \varphi_B \circ \phi_{AB} \circ \varphi_A$, that are locally defined in neighbourhoods of the connections. The maps are neither defined at all points of the walls $\mathcal{W}_e$ and tops $\mathcal{T}_e$ of the cylinders, nor for the whole neighbourhood R_1, but roughly speaking, they are as in figure 4:

$$\varphi_A : \mathcal{W}^+_A \to \mathcal{T}_A \qquad \varphi_B : \mathcal{T}_B \to \mathcal{W}^+_B,$$

where

$$\mathcal{W}^+_e = \{(r, \theta, z)\ r = r_e \text{ and } z > 0\}, \qquad e = A, B,$$

and

$$\phi_{AB} : \mathcal{T}_A \to \mathcal{T}_B \qquad \phi_{BA} : \mathcal{W}_B \to \mathcal{W}_A.$$

A similar return map can be defined when the flow goes through the bottom, $\mathcal{B}_e$, of the cylinders with analogous results. First we explore the transition $\Phi = \varphi_B \circ \phi_{AB} \circ \varphi_A$, from $\mathcal{W}^+_A$ to $\mathcal{W}^+_B$.

For $e = A, B$ we parametrize the cylinder walls $\mathcal{W}_e$, $e = A, B$ by $(x, y) \mapsto (r_e, x, y) = (r_e, \theta, z)$ with $x \in \mathcal{W}_{e_0}$ being the azimuthal direction θ. The cylinder tops, $\mathcal{T}_e$, are parametrized in polar coordinates by $(r, \theta) \mapsto (r, \theta, z_e), r > 0$. For $p = (x_0, 0) \in \mathcal{W}_{e_0}$ we define a *rectangle centred at* p as the set

$$R_p = \{(x, u) : -w \leqslant x - x_0 \leqslant w \text{ and } -y_0 \leqslant u \leqslant y_0\} \subset \mathcal{W}_e,$$

with height $2y_0$, $0 < y_0 < z_e$, and width $2w$, $0 < w \ll \pi$. Their interiors form a basis for an open cover of $\mathcal{W}_{e_0}$. The *positive rectangle centred at* p will be $R_p^+ = R_p \cap \mathcal{W}_e^+$.

Proposition 2. *Let X be a vector field satisfying (H0)–(H6). Let $p \in \mathcal{W}_{A_0}$ and $q \in \mathcal{W}_{B_0}$ be two points in the connections $[B \to A]$ (not necessarily in the same connection) and let $\Phi = \varphi_B \circ \phi_{AB} \circ \varphi_A$. Given rectangles $R_p \subset \mathcal{W}_A$ centred at p and $R_q \subset \mathcal{W}_B$ centred at q, then $\Phi(R_p^+) \cap R_q \neq \emptyset$. Moreover, assuming ϕ_{AB} is the identity, in suitable coordinates in R_p and R_q, there are constants c_1, c_2, with $c_1 < 0$, such that*

$$\Phi(x, y) = (\Phi_1(x, y), \Phi_2(x, y)) = (x + c_1 \ln y + c_2, y).$$

Proof. Choose coordinates (x, y) in $\mathcal{W}_A$ as above, with p at the origin $x = y = 0$. It is sufficient to show the result for R_p and R_q, arbitrary rectangles centred at p and q, respectively.

Since the flow has been linearized in N_e, and using (H1) the expressions for φ_e in these coordinates are:

$$\varphi_A(x, y) = \left(r_A \left(\frac{y}{z_A} \right)^{-\alpha_A/\lambda_A}, x - \frac{\beta_A}{\lambda_A} \ln \left(\frac{y}{z_A} \right) \right) = (r, \theta), \tag{5}$$

$$\varphi_B(r, \theta) = \left(\theta - \frac{\beta_B}{\alpha_B} \ln \left(\frac{r}{r_B} \right), z_B \left(\frac{r}{r_B} \right)^{-\lambda_B/\alpha_B} \right) = (x, y). \tag{6}$$

With the simplifying assumptions $r_A = r_B$, $z_A = z_B = z_1$ and ϕ_{AB} the identity map, we get the coordinates (x, y) of Φ,

$$\Phi(x, y) = (\Phi_1(x, y), \Phi_2(x, y)) = (x + c_1 \ln y + c_2, c_4 y^{c_3}), \tag{7}$$

where

$$c_1 = \frac{\alpha_A \beta_B - \beta_A \alpha_B}{\lambda_A \alpha_B}, \qquad c_2 = -c_1 \ln z_1, \qquad c_3 = \frac{\alpha_A \lambda_B}{\lambda_A \alpha_B}, \qquad c_4 = z_1^{(1-c_3)}.$$

By hypotheses (H1), (H2), $c_1 < 0$ and by (H1), (H3) we have $c_3 = 1$, $c_4 = 1$. Hence, $\Phi(x, y) = (x + c_1 \ln y + c_2, y)$. Thus, Φ maps a vertical segment (x_1, u), $0 < u < y_0$ on the wall $\mathcal{W}_A$ into a helix that winds around $\mathcal{W}_B$ and accumulates on the circle $\mathcal{W}_{B_0}$ as $u \to 0$ (see figure 5). The image of another vertical segment, $\Phi(x_2, u)$, $0 < u < y_0$, may be obtained from that of the first segment by displacing the helix around the cylinder by an angle $(x_2 - x_1)$.

A rectangle $[x_1, x_2] \times [K y_2, y_2]$ in $\mathcal{W}_A^+$ with $y_2 > 0$, $0 < K < 1$ is mapped into the region delimited by two helices. Its image makes a complete turn around the cylinder when $K = \mathrm{e}^{2\pi/c_1} = \mathrm{e}^{-\pi\lambda_A/\beta_A}$. Thus the image of a rectangle $R_p^+ = [-w, w] \times [0, y_0]$ meets any neighbourhood of q.

If ϕ_{AB} is any orientation-preserving diffeomorphism, then the geometry of Φ is the same: a vertical segment in $\mathcal{W}_A$ is still mapped by Φ into a helix around $\mathcal{W}_B$ that accumulates on the circle $\mathcal{W}_{B_0}$. Although expression (7) no longer holds, the proof is the same if ϕ_{AB} is linear.

If ϕ_{AB} is not linear, the estimate $K = \mathrm{e}^{2\pi/c_1}$ no longer guarantees a complete turn for the image. However, for each choice of $K < \mathrm{e}^{2\pi/c_1}$ there is a small enough value of $y_2 > 0$ such that the image of $[x_1, x_2] \times [K y_2, y_2]$ in $\mathcal{W}_A^+$ makes a complete turn around the cylinder. □

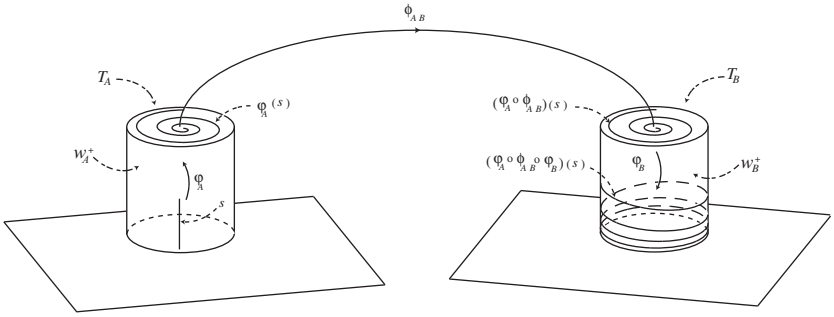

Figure 5. Geometry of $\Phi = \varphi_B \circ \phi_{AB} \circ \varphi_A$.

Note that if we had taken the rotation in N_B with the opposite orientation, then the two rotations in φ_A and φ_B would cancel out and we would obtain the identity map as the first order approximation of Φ. Our choice of orientation reflects what is observed numerically in Field's example.

Note also that, even though it is possible to change coordinates in $\mathcal{T}_A$ and $\mathcal{T}_B$ so that ϕ_{AB} is the identity, this destroys the forms (5) and (6) of φ_A and φ_B.

We adapt the definition of horizontal and vertical strips in Guckenheimer and Holmes [17], chapter 5, to serve our purposes.

In a rectangle $R = [-w, w] \times [-h, h]$, a *vertical curve* $x = v(y)$ is a curve for which

$$-w \leqslant v(y) \leqslant w \quad |v(y_1) - v(y_2)| \leqslant \mu |y_1 - y_2| \qquad \text{in } -h \leqslant y_1 \leqslant y_2 \leqslant h$$

for some $0 < \mu < 1$. Similarly, a *horizontal curve* $y = h(x)$ is one for which

$$-h \leqslant h(x) \leqslant h \quad |h(x_1) - h(x_2)| \leqslant \mu |x_1 - x_2| \qquad \text{in } -w \leqslant x_1 \leqslant x_2 \leqslant w$$

for some $0 < \mu < 1$.

Given two nonintersecting vertical curves $v_1(y) < v_2(y)$, $y \in [-h, h]$ and two nonintersecting horizontal curves $h_1(x) < h_2(x)$, $x \in [-w, w]$, we define *vertical* and *horizontal strips*, respectively, as

$$V = \{(x, y) : x \in [v_1(y), v_2(y)], y \in [-h, h]\},$$

$$H = \{(x, y) : x \in [-w, w],\ y \in [h_1(x), h_2(x)]\}.$$

Note that, in some instances, we shall use the generic word *strip* for a subrectangle.

Proposition 3. *Let X be a vector field satisfying (H0)–(H6). Let $p_1, p_2 \in \mathcal{W}_{A_0}$ be points in the connections $[B \to A]$ (in the same or in different connections). Then, for sufficiently small rectangles $R_{p_j} \subset \mathcal{W}_A$ centred at p_j of width w_j, $j = 1, 2$, there are two sequences (z_i) and (y_i) with $\lim_{i\to\infty} z_i = 0$ and $0 < y_{i+1} < z_{i+1} < y_i < z_i$ such that the transition map $\Psi = \phi_{BA} \circ \varphi_B \circ \phi_{AB} \circ \varphi_A$ is well defined in the strips $[-w_1, w_1] \times [y_i, z_i] \subset R_{p_1}$ and Ψ maps each horizontal strip in R_{p_1} into a vertical strip across R_{p_2}. Moreover, assuming ϕ_{AB} is the identity and ϕ_{BA} a rotation of $\pi/2$, in suitable coordinates in R_{p_1} and R_{p_2} we may take in each strip*

$$\Psi(x, y) = (-y, x + c_1 \ln(y) + c_2) = (\tilde{x}, \tilde{y}) \qquad (\text{mod } 2\pi),$$

where the constants $c_1 < 0$ and c_2 are the same as in proposition 2.

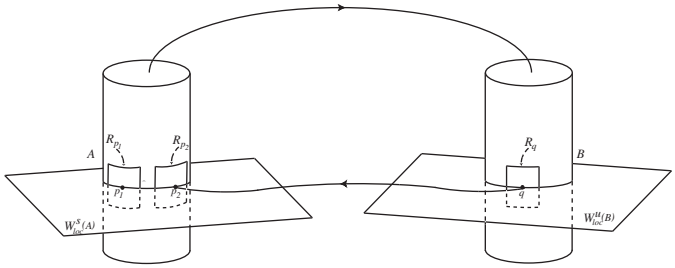

Figure 6. Geometrical setting of proposition 3.

Proof. Let $q \in \mathcal{W}_{B_0}$ be such that the trajectory through q arrives at p_2 (see figure 6). We choose local coordinates (x, y) in $\mathcal{W}_A$ and $\mathcal{W}_B$ with p_1 and q at the origin, so $R_{p_1} = [-w_1, w_1] \times [-h_1, h_1]$ for some $h_1 > 0$.

Let $2h_2$ and $2w_2$ be the height and width, respectively, of R_{p_2} and consider a rectangle $R_q \in \mathcal{W}_B$ centred at q, of height $2h_3 = 2w_2$ and width $2w_3 = 2h_2$.

First, we obtain strips in $R^+_{p_1}$ that are mapped by Φ across R_q (see figure 7). Using the expression (7) for Φ, let z_i be the largest value of u such that $\Phi_1(w_1, u) = -w_3 \pmod{2\pi}$ with $0 < u < y_{i-1}$ (for $i = 1$ take $0 < u < \min\{h_1, h_3\}$). This value always exists, since $u \mapsto \Phi(w_1, u)$ makes a complete turn around the cylinder when $Ky_{i-1} \leqslant u \leqslant y_{i-1}$ as remarked at the end of the proof of proposition 2. Now we take y_i as the largest value of u such that $\Phi_1(-w_1, u) = w_3 \pmod{2\pi}$ with $0 < u < z_i$. Thus Φ maps the horizontal strip $[-w_1, w_1] \times [y_i, z_i]$ in R_{p_1} into the strip $[-w_3 - 2w_1, w_3 + 2w_1] \times [y_i, z_i]$ in $\mathcal{W}_B$. This image contains the horizontal strip $[-w_3, w_3] \times [f_1(x), f_2(x)]$ in R_q, where $f_1(x) = \exp(x + w_1 - c_2)/c_1$ and $f_2(x) = \exp(x - w_1 - c_2)/c_1$.

We may assume, by shrinking the rectangles if necessary, that R_q is contained in a flow-box around the trajectory connecting q to p_2. The map ϕ_{BA} is well defined in R_q. It follows that Ψ is well defined in the strips $[-w_1, w_1] \times [y_i, z_i] \subset R_{p_1}$.

Take coordinates $(\tilde{x}, \tilde{y})$ in $\mathcal{W}_A$ near p_2 with p_2 at the origin. As a simplification, we assume ϕ_{BA} is a rotation of $\pi/2$ and take q at the origin of the coordinates in $\mathcal{W}_B$, to obtain using (7)

$$\Psi(x, y) = \left(-y, x + c_1 \ln\left(\frac{y}{z_1}\right)\right) = (\tilde{x}, \tilde{y}) \qquad (\text{mod } 2\pi), \tag{8}$$

where $c_1 \neq 0$ as before. The expression for Ψ is well defined only when $\Phi(x, y)$ is near q and its coordinates are both defined modulo 2π. Since R_{p_2} is the image by ϕ_{BA} of R_q and $h_2 = w_3$, a strip $[-w_1, w_1] \times [y_i, z_i] \subset R_{p_1}$ is mapped by Ψ across R_{p_2}.

The proof holds for any rotation of an angle between 0 and π with a more complicated expression for Ψ. □

6.1. Switching at nodes

We are now able to describe the dynamics in a neighbourhood of a network such as the quotient network of subsection 5.1. We start with switching at the nodes. The result is implicit in propositions 2 and 3.

Theorem 4. *There is switching at the two nodes of a network of a vector field satisfying (H0)–(H6).*

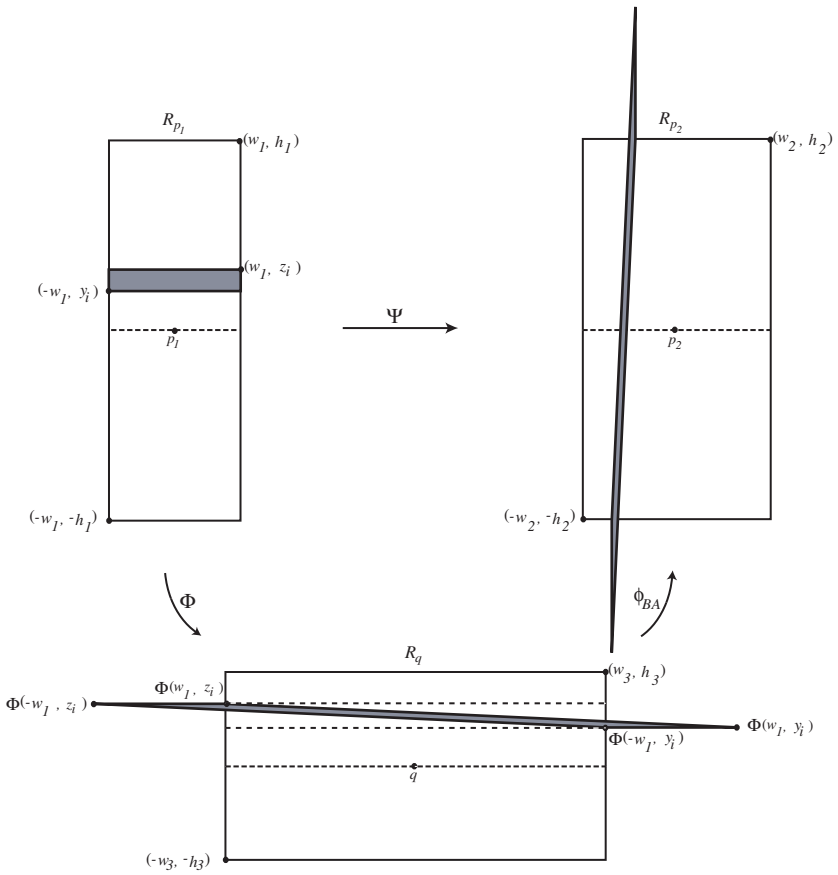

Figure 7. Geometry of the return map in proposition 3.

Proof. First we show that switching at A follows directly from (H0), (H1) and (H6). Let q be a point in one of the connections $[B \to A]$. Any sufficiently small neighbourhood of q is contained in a flow-box around the connection and so it is mapped by the flow into $\mathcal{W}_B$ either in small positive time or in small negative time, and so we may suppose $q \in \mathcal{W}_B$. Any neighbourhood of q contains a connected arc N_0 such that $q \in N_0 \subset \mathcal{W}_{B_0}$. The transversality of the intersection of the two-manifolds implies that there are points in N_0 that are mapped by the flow into $\mathcal{W}_A^+$ (and then follow the connections $[A \to B]$ through $\mathcal{T}_A, \mathcal{T}_B$) and also points that go to $\mathcal{W}_A^-$, and then follow the flow through $\mathcal{B}_A, \mathcal{B}_B$. Thus, there is switching at A.

Next, we use (H0), (H1), (H4) and (H5) to obtain switching at B. Points in a neighbourhood of the connection from $\mathcal{T}_A$ to $\mathcal{T}_B$ are mapped by the flow into a neighbourhood of the origin of $\mathcal{T}_B$. Consider any ray (r, θ_0) in $\mathcal{T}_B$, θ_0 fixed, $0 < r < r_0$. Using (6), it is easy to see that this ray is mapped by φ_B into a helix, similar to those in figure 5, that accumulates on all of $\mathcal{W}_{B_0}$ as $r \to 0$. For instance, the points $(r, 0) \in \mathcal{T}_B$ are mapped by φ_B into

$$\varphi_B(r, 0) = \left(\frac{\beta_B}{\alpha_B} \ln r + c, z_B \left(\frac{r}{r_B} \right)^{-\lambda_B/\alpha_B} \right) = (x, y),$$

where the coordinate x in the cylinder wall $\mathcal{W}_B$ is taken modulo 2π. In particular, for each of the m connections $[B \to A]$ there are points $(r, 0) \in \mathcal{T}_B$ that follow the given connection.

For trajectories near $[A \to B]$ that go from $\mathcal{B}_A$ to $\mathcal{B}_B$ the same result holds, with the same proof. □

Note that to establish switching at A, we have exhibited trajectories that lie in $W^u(B)$ and therefore these trajectories do not follow the network in negative time. This provides an example of the fact that switching at all nodes does not guarantee switching on the network. We are not using all the information available, as will be clear in subsection 6.4.

6.2. Horseshoe geometry

Now we address the special case of points in a neighbourhood of a connection $[B \to A]$ that return to a neighbourhood of the same connection. This corresponds to the case $p_1 = p_2$ in proposition 3.

The next result shows that the return map Ψ has the geometrical behaviour of a horseshoe. We use the same coordinates as in the proofs of propositions 2 and 3. In these coordinates we have obtained an expression for Ψ and the expression is the same, independent of the connection considered.

Corollary 5. *Let X be a vector field satisfying (H0)–(H6). Let $p \in \mathcal{W}_{A_0}$ be a point in one of the connections $[B \to A]$ and R_p a rectangle centred at p. Then, there is a rectangle $R = [-\nu, \nu] \times [y, z] \subset R_p$ with $\nu > 0$ and $z > y > 0$ such that there are two horizontal strips $H_i \subset R$, $i = 1, 2$ such that Ψ is well defined in each strip H_i and $\Psi(H_i) \cap R$ is a vertical strip across R.*

Proof. Reducing R_p if necessary, suppose it is sufficiently small so that we may apply proposition 3 with $p = p_1 = p_2$, $R_p = R_{p_1} = R_{p_2}$ and $w = w_1 = w_2$ to obtain two sequences (z_j) and (y_j). The result follows from proposition 3. □

We point out that the horseshoe in corollary 5 lies between heights y and z. Applying this corollary to another rectangle R_p of height less than y, we obtain another horseshoe, and therefore there are an infinite number of horseshoes accumulating on the connection.

6.3. Hyperbolicity

Let Ψ be the transition map from a strip contained in a rectangle centred at a connection point into another rectangle centred at another connection point.

In this section we show that Ψ, with the expression given in proposition 3, is hyperbolic in the sense defined below. When Ψ is a return map on a rectangle centred at a connection point, i.e. when the two connection points are the same, this guarantees that the invariant sets of the Poincaré map Ψ are Cantor sets, where the dynamics is conjugated to a shift on infinite sequences of two symbols; otherwise we can only guarantee semi-conjugacy. Hyperbolicity of the transition map Ψ between different rectangles is important for establishing persistence of the dynamics and switching on the network, and will be used in subsection 6.4.

We say that Ψ is *hyperbolic* at a point (x, y) if both Ψ and Ψ^{-1} are well defined at (x, y) and if there is δ, $0 < \delta < 1$ such that, in suitable coordinates, the derivatives $D\Psi_{|(x,y)}$ and $D\Psi^{-1}_{|(x,y)}$ satisfy the following.

- The sector-bundle $S^u = \{(v_1, v_2) : |v_1| < \delta |v_2|\}$ is invariant by $D\Psi_{|(x,y)}$, i.e. $D\Psi_{|(x,y)}(S^u) \subset S^u$.
- The sector-bundle $S^s = \{(v_1, v_2) : |v_2| < \delta |v_1|\}$ is invariant by $D\Psi^{-1}_{|(x,y)}$, i.e. $D\Psi^{-1}_{|(x,y)}(S^s) \subset S^s$.

- For $(v_1, v_2) \in S^u$, if $D\Psi_{|(x,y)}(v_1, v_2) = (w_1, w_2)$, then $|w_2| \geqslant (1/\delta)|v_2|$.
- For $(v_1, v_2) \in S^s$, if $D\Psi^{-1}_{|(x,y)}(v_1, v_2) = (u_1, u_2)$, then $|u_1| \geqslant (1/\delta)|v_1|$.

Theorem 6. *Assume hypotheses (H0)–(H6) hold. Let p_1, $p_2 \in \mathcal{W}_A$ be connection points and let R_{p_i} be open rectangles of height $2h \leqslant -c_1$ centred at p_i. Then, with the expression given in proposition 3, the Poincaré map Ψ from R_{p_1} to R_{p_2} is hyperbolic at all points in R_{p_1} where it is well defined.*

Proof. Let $p = p_1$. It is sufficient to verify hyperbolicity at points (x, y) in the strips of proposition 3, but we will consider any point (x, y) in R_p.

Using (8) at a point $(x, y) \in R_p$, we get

$$D\Psi_{|(x,y)} = \begin{bmatrix} 0 & -1 \\ 1 & \dfrac{c_1}{y} \end{bmatrix}, \qquad D\Psi^{-1}_{|(x,y)} = \begin{bmatrix} \dfrac{c_1}{y} & 1 \\ -1 & 0 \end{bmatrix}.$$

Note that the symmetry $(w_1, w_2) \mapsto (w_2, w_1)$ transforms $D\Psi$ into $D\Psi^{-1}$. Therefore all results proved for $D\Psi$ hold for $D\Psi^{-1}$ with coordinates interchanged.

We obtain explicit expressions for the eigenvalues and eigenvectors of $D\Psi$ in lemma 7. The invariance of sector-bundles is shown in lemma 8 and the expansion property in lemma 9. □

Lemma 7. *Under the conditions of theorem 6, the derivative $D\Psi_{|(x,y)}$ at a point $(x, y) \in R_p$, such that $0 < y < -c_1/2$, has real eigenvalues μ_u and μ_s satisfying $\mu_u < -1 < \mu_s < 0$ with eigenvectors $v_u = (-\mu_s, 1)$ corresponding to μ_u, and $v_s = (1, -\mu_s)$ corresponding to μ_s.*

Proof. The eigenvalues of $D\Psi_{|(x,y)}$ can be computed directly:

$$\mu_u = \frac{c_1}{2y} - \sqrt{\left(\frac{c_1}{2y}\right)^2 - 1} \qquad \text{and} \qquad \mu_s = \frac{c_1}{2y} + \sqrt{\left(\frac{c_1}{2y}\right)^2 - 1}.$$

Since $0 < y < -c_1/2$, the two eigenvalues are real. $\mu_s < 0$ follows from

$$\sqrt{\left(\frac{c_1}{2y}\right)^2 - 1} < \left|\frac{c_1}{2y}\right| = \frac{-c_1}{2y}.$$

Since $c_1/2y < -1$, it follows that $\mu_u < -1$. On the other hand, it is easy to check that $\mu_s > -1$ is equivalent to $c_1/2y < -1$. An eigenvector of $D\Psi_{|(x,y)}$ corresponding to the eigenvalue μ has the form $(-1/\mu, 1)$. The expressions for v_u and v_s follow since $\mu_s\mu_u = \det D\Psi_{|(x,y)} = 1$. □

From the expressions for the eigenvalues it follows that

$$\lim_{y\to 0} \mu_u = -\infty \qquad \text{and} \qquad \lim_{y\to 0} \mu_s = 0$$

and that, moreover, the eigenspaces define limit directions:

$$\lim_{y\to 0} \frac{v_u}{|v_u|} = (0, 1) \qquad \text{and} \qquad \lim_{y\to 0} \frac{v_s}{|v_s|} = (1, 0).$$

Choose the invariant sectors S^u, near the vertical direction, and S^s, near the horizontal direction, and define them as explained earlier.

Lemma 8. *With the hypotheses of theorem 6, with* $-\mu_s < \delta < 1 < -\mu_u$ *and* $(x, y) \in R_p^+$, *then* $D\Psi_{|(x,y)}(S^u) \subset S^u$ *and* $D\Psi^{-1}_{|(x,y)}(S^s) \subset S^s$.

Proof. We show the invariance of S^u; the result for S^s follows by symmetry. It is sufficient to show that $(\delta, 1)$ and $(-\delta, 1)$ are mapped by $D\Psi_{|(x,y)}$ inside the same component of S^u—the invariance follows by linearity.

Since $(x, y) \in R_p^+$ it follows that $d = c_1/2y < -1$. With this notation, the eigenvalues of $D\Psi_{|(x,y)}$ are $\mu_s = d + \sqrt{d^2 - 1}$ and $\mu_u = d - \sqrt{d^2 - 1}$.

Consider first the image of $(\delta, 1)$, given by $(v_1, v_2) = (-1, \delta + 2d)$. We have the relation that $|v_1| < \delta|v_2|$ since this inequality is equivalent to $\delta^2 + 2d\delta + 1 < 0$ which occurs if and only if $-\mu_s < \delta < -\mu_u$. Therefore (v_1, v_2) lies in S^u.

Analogously, we show that the image of $(-\delta, 1)$, given by $(w_1, w_2) = (-1, -\delta + 2d)$, lies in S^u.

Finally, since both v_2 and w_2 are negative, they lie in the same component of S^u, proving the result. □

Lemma 9. *Denote* $D\Psi_{|(x,y)}(v_1, v_2)$ *by* (ω_1, ω_2) *and* $D\Psi^{-1}_{|(x,y)}(u_1, u_2)$ *by* (v_1, v_2). *Under the conditions of theorem 6, if* $-\mu_s < \delta < 1 < -\mu_u$, *for* $(x, y) \in R_p^+$, $(v_1, v_2) \in S^u$ *and* $(u_1, u_2) \in S^s$, *then* $|w_2| \geqslant (1/\delta)|v_2|$ *and* $|v_1| \geqslant (1/\delta)|u_1|$.

Proof. We show the result for S^u and $D\Psi$, and the other case follows from symmetry. We have $D\Psi_{|(x,y)}(v_1, v_2) = (\omega_1, \omega_2) = (-v_2, v_1 + 2dv_2)$ with $d = c_1/2y$. The expansion condition is

$$|v_1| < \delta|v_2| \implies \delta|v_1 + 2dv_2| = \delta|\omega_2| \geqslant |v_2|.$$

For this it is sufficient to show that $(\delta, 1)$ and $(-\delta, 1)$ lie in the same component of the sector defined by $\delta|v_1 + 2dv_2| \geqslant |v_2|$.

Since $\delta < -\mu_u = -d + \sqrt{d^2 - 1} < -2d$, then $\delta + 2d < 0$. For $(v_1, v_2) = (\delta, 1)$ we obtain

$$\delta|v_1 + 2dv_2| - |v_2| = \delta|\delta + 2d| - 1 = -(\delta^2 + 2d\delta + 1).$$

The roots of $\delta^2 + 2d\delta + 1 = 0$ are $-\mu_s$ and $-\mu_u$ and so $-(\delta^2 + 2d\delta + 1) > 0$ if $-\mu_s < \delta < -\mu_u$. It follows that $(\delta, 1)$ lies in the $v_2 > 0$ component of the sector.

Analogously, we prove that $(-\delta, 1)$ lies in the $v_2 > 0$ component of the sector. □

Corollary 5 and the case $p_1 = p_2 = p$ of theorem 6 guarantee the existence of horseshoe dynamics near the heteroclinic cycles in the two-node network. Near each cycle there is a suspended horseshoe that meets $\mathcal{W}_A$ in a Cantor set. See Guckenheimer and Holmes [17], chapter 5 and Wiggins [28], chapter 2.

Remark. By (H6) there is a flow-invariant neighbourhood of the connection through p that meets $\mathcal{W}_A$ in R_p. Using (H5), and by the stronger version of switching at A in the proof of theorem 10, it follows that the suspended horseshoe is captured by the union of N_A, N_B and the two flow-invariant neighbourhoods of the connections.

6.4. Switching on the network

The main result in this paper can now be proved: switching on a network like the quotient network of subsection 5.1. The proof follows the construction of proposition 3 as a more complicated version of the proof of corollary 5.

Theorem 10. *There is switching on any network of a vector field satisfying (H0)–(H6).*

Proof. Given a neighbourhood N_Σ of the network Σ, we may take the neighbourhoods N_A, N_B of A and B as before, restricting them to intersections with N_Σ if necessary.

Let $p_1, \ldots, p_{\mathsf{m}}$ be representative points in the connections $[B \to A]$, and let ϱ_+, ϱ_- be points in the two connections $[A \to B]$. Using (H5) and (H6) we may take the p_i in $\mathcal{W}_{A_0}$, ϱ_+ in $\mathcal{T}_A$ and ϱ_- in $\mathcal{B}_A$ i.e. $\{p_1, \ldots, p_{\mathsf{m}}\} = \mathcal{W}_{A_0} \cap W^u_{\mathrm{loc}}(B)$, $\{\varrho_+\} = W^u_{\mathrm{loc}}(A) \cap \mathcal{T}_A$ and $\{\varrho_-\} = W^u_{\mathrm{loc}}(A) \cap \mathcal{B}_A$. In the coordinates we are using, ϱ_+ is the origin of $\mathcal{T}_A$.

A path in Σ visits the nodes A and B alternately since there are no connections from a node to itself. Thus, paths in Σ may be represented by sequences $(a_n)_{n\in\mathbf{Z}}$ where $a_{2n} \in \{p_1, \ldots, p_{\mathsf{m}}\}$ and $a_{2n+1} \in \{\varrho_+, \varrho_-\}$.

The following stronger version of switching at the node A holds. Given $h > 0$, with $h < z_A$, consider the cylinder of height h in $\mathcal{W}^+_A$; in coordinates (x, y) on $\mathcal{W}^+_A$ this is $\{(x, y) : 0 \leqslant y \leqslant h\}$. Using the expression for φ_A in the proof of proposition 2, it is easy to see that this cylinder is mapped inside a disk of radius $r(h)$ in $\mathcal{T}_A$ such that $\lim_{h\to 0} r(h) = 0$ (actually, $r(h)$ is an increasing function of h, with $r(0) = 0$). Similarly, a cylinder of height h in $\mathcal{W}^-_A$ is mapped inside a small disc in $\mathcal{B}_A$.

Let R_{p_j} be the rectangle centred at p_j of height $2h$ and width $2w$. Points in $R^+_{p_j}$ follow paths corresponding to the partial sequence $a_0, a_1 = p_j, \varrho_+$ and those on $R^-_{p_j}$ follow $a_0, a_1 = p_j, \varrho_-$.

By proposition 3, if h and w are small enough, then there is a strip $S^+_{j1} = [-w, w] \times [y_1, z_1] \in R^+_{p_j}$ where the transition Ψ-to-R_{p_1} is well defined and maps the strip across R_{p_1}. Then proposition 3 may be applied to the rectangle centred at p_j of width $2w$ and height $2y_1$, to obtain a second strip $S^+_{j2} = [-w, w] \times [y_2, z_2] \in R^+_{p_j}$ with $z_2 < y_1$ that is mapped across R_{p_2}. Repeating the procedure, we obtain in each $R^+_{p_j}$, m strips S^+_{ji} where the return to $\mathcal{W}_A$ going through $\mathcal{T}_A$ is well defined and maps S^+_{ji} across R_{p_i}. Another m strips S^-_{ji} in $R^-_{p_j}$ may be obtained, where the return to $\mathcal{W}_A$ going through $\mathcal{B}_A$ is well defined and maps S^-_{ji} across R_{p_i}. As in the usual horseshoe construction, points in the strips S^+_{ji} follow paths corresponding to the partial sequence $a_0, a_1, a_2 = p_j, \varrho_+, p_i$ and those on S^-_{ji} follow $a_0, a_1, a_2 = p_j, \varrho_-, p_i$.

If $2h < -c_1$, then by theorem 6, the Poincaré map Ψ is hyperbolic in all the strips. It follows that the set

$$\Lambda = \bigcap_{k\in\mathbf{Z}} \left(\bigcup_{\substack{j,i=1 \\ \varepsilon=\pm}}^{\mathsf{m}} \Psi^k(S^\varepsilon_{ji}) \right)$$

is a Cantor set of points where the return to $\cup R_{p_j}$ is well defined in forward and backward time for arbitrarily large times. The dynamics of Ψ in the invariant set Λ is conjugated to a full shift on the $2\mathsf{m}$ symbols (p_j, ϱ_l) that represent paths in Σ. Each point in Λ will correspond to a unique path on the network that it follows in forward and backward time. If hyperbolicity does not hold, semi-conjugacy of the dynamics of Ψ in Λ to a full shift ensures the existence of a path, possibly not unique. This establishes the switching. □

7. Lifted dynamics

In this section we describe the consequences of the results obtained in the previous section to the dynamics of the original flow. We discuss how to lift the dynamics from the quotient to the original network of equilibria.

For clarity next we list the attributes of the original vector field X that are going to be used here. All these have already been discussed for the vector field (1) with parameters satisfying (3), and the network of equilibria Σ given by the first two rows of table 2.

♠ The finite group Γ acts orthogonally on S^3, with a subgroup G acting freely on S^3.
X is a Γ-equivariant vector field on S^3 with a Γ-invariant network of equilibria Σ.
For any two nodes n_1, n_2 in Σ there is at most one trajectory connecting n_1 to n_2 in Σ.
The only element of G that fixes a node in Σ is the identity.

Under these assumptions we may lift theorem 4 to the original network.

Corollary 11. *Let X be a vector field on S^3 with a network of equilibria Σ satisfying ♠ and suppose the quotient network $\tilde{\Sigma} = \Sigma/G$ on S^3/G for the quotient vector field $\tilde{X} = X/G$ satisfies (H0)–(H6). Then there is switching at each node of Σ.*

Proof. This follows from the same arguments used in the proof of theorem 4, after lifting propositions 2 and 3 to the original vector field. Instead of repeating the arguments we note that since the action of G is free, then for each node n in Σ the natural projection $\pi : S^3 \longrightarrow S^3/G$ is a diffeomorphism that maps a neighbourhood of n onto a neighbourhood of $\pi(n)$. Local behaviour of the flow, like switching at node n, is preserved by π and by its local inverse. □

Switching on the network is not a local property and thus its lifting requires more work. We start by lifting paths on the network.

Lemma 12. *Let X be a vector field on S^3 with a network of equilibria Σ satisfying ♠ and let $\tilde{\Sigma} = \Sigma/G$ be the quotient network on S^3/G for the quotient vector field $\tilde{X} = X/G$. Then any two paths on Σ that coincide in one node and that drop down to the same path on $\tilde{\Sigma}$ are the same.*

Proof. Two paths $(c_j)_{j\in\mathbf{Z}}$ and $(d_j)_{j\in\mathbf{Z}}$ on Σ drop down to the same path if for all j we have $\pi(c_j) = \pi(d_j)$, i.e. for each $j \in \mathbf{Z}$ there is $\gamma_j \in G$ such that $c_j = \gamma_j \cdot d_j$. If $c_j = [n_{j-1} \to n_j]$ and $d_j = [m_{j-1} \to m_j]$, then in particular $n_j = \gamma_j \cdot m_j$.

Suppose that $n_k = m_k$ for some $k \in \mathbf{Z}$. Then $n_k = \gamma_k \cdot m_k = m_k$ and thus, by hypothesis, γ_k is the identity. Therefore $[n_k \to n_{k+1}] = [m_k \to m_{k+1}]$ and in particular $n_{k+1} = m_{k+1}$.

The same argument shows that if $n_k = m_k$ then $[n_{k-1} \to n_k] = [m_{k-1} \to m_k]$ and the result follows by induction. □

Thus any path on $\tilde{\Sigma}$ lifts to a finite number of paths on Σ. If $(c_j)_{j\in\mathbf{Z}}$ and $(d_j)_{j\in\mathbf{Z}}$ are two such paths, then either they coincide or for each $j \in \mathbf{Z}$ the connections c_j and d_j are disjoint. For instance, for the network of equilibria given by the first two rows of table 2, consider the case of a periodic path corresponding to a simple cycle in the quotient network, given by one choice of connection in $[A \to B]$ and another in $[B \to A]$. For example, we may choose the connections $G \cdot [a \to b]$ and $G \cdot [b \to sa]$. This cycle lifts to two disjoint simple cycles in the original network of equilibria. With our choice of connections it either lifts to the cycle

$$a \to b \to sa \to sb \to s^2a \to s^2b \to s^3a \to s^3b \to s^4a \to s^4b \to s^5a = a,$$

or to a similar cycle with a minus sign everywhere. Any other path in Σ that drops to the same cycle in $\tilde{\Sigma}$ can be obtained from one of these two by a shift. Note that the cycle $G \cdot [a \to -b]$ and $G \cdot [-b \to sa]$ lifts to a single cycle of twice the length, visiting all the saddles in Σ.

Theorem 13. *Let X be a vector field on S^3 with a network of equilibria Σ satisfying ♠ and suppose the quotient network $\tilde{\Sigma} = \Sigma/G$ on S^3/G for the quotient vector field $\tilde{X} = X/G$ satisfies (H0)–(H6). Then there is a suspended horseshoe in any neighbourhood of each cycle in Σ.*

Proof. When we iterate Ψ we are following along a simple cycle in the quotient network: by corollary 5 and theorem 6 the quotient flow is a suspended horseshoe. From lemma 12 it follows that the simple cycle lifts to a finite number of disjoint simple cycles in Σ. By the remark at the end of subsection 6.3, the suspended horseshoe is contained in flow-invariant neighbourhoods of the connections. The suspended horseshoe lifts to a suspended horseshoe that follows the lifted cycle. □

Theorem 14. *Let X be a vector field on S^3 with a network of equilibria Σ satisfying ♠ and suppose the quotient network $\tilde{\Sigma} = \Sigma/G$ on S^3/G for the quotient vector field $\tilde{X} = X/G$ satisfies (H0)–(H6). Then there is switching in Σ.*

Proof. Without loss of generality, consider a Γ-invariant neighbourhood N_Σ of Σ, and take a Γ-invariant set of neighbourhoods of the nodes in Σ. These drop down to neighbourhoods $N_{\tilde{\Sigma}}$, N_A and N_B of $\tilde{\Sigma}$, A and B, respectively. The results of section 6 hold in these neighbourhoods, reducing them if necessary. Again, without loss of generality, consider a Γ-invariant set of representative points of the connections in Σ and a Γ-invariant set of their neighbourhoods, that drop down to representative points q_j, $j = 1, \ldots, 10$ of all the ten connections in $\tilde{\Sigma}$ and neighbourhoods N_{q_j} of the q_j.

Start with a path $([m_{j-1} \to m_j])_{j\in\mathbf{Z}}$ on Σ that drops down to a path $([M_{j-1} \to M_j])_{j\in\mathbf{Z}}$ on $\tilde{\Sigma}$.

By theorem 10 the quotient path can be shadowed, inside $N_{\tilde{\Sigma}}$, by a trajectory $\tilde{x}(t)$ of the quotient vector field $\tilde{X}$. More precisely, if p_j is the representative point $p_j \in \{q_1, \ldots, q_{10}\}$ that lies on the connection $[M_{j-1} \to M_j]$, then there are sequences (t_j), (s_j), $j \in \mathbf{Z}$ with $t_{j-1} < s_j < t_j$, such that $\tilde{x}(s_j) \in U_{p_j}$ and $\tilde{x}(t_j) \in U_{M_j}$.

Let x_0 be a point in the neighbourhood of $m_0 \in S^3$ satisfying $\pi(x_0) = \tilde{x}(t_0) \in U_{M_0}$, and let $x(t)$ be the trajectory of X satisfying $x(t_0) = x_0$, and thus $\pi(x(t)) = \tilde{x}(t)$. Using hypotheses (H5) and (H6), theorem 10 can be stated and proved with flow-invariant neighbourhoods of the connections. The proof is complete since, by arguments like those in the proof of lemma 12, $x(t)$ follows the path $([m_{j-1} \to m_j])_{j\in\mathbf{Z}}$. □

8. Conclusions

This paper contributes to a better understanding of the dynamics near a specific type of heteroclinic network for a vector field on a three-dimensional manifold. Structural stability is ensured by hyperbolicity around the nodes and by the type of connection between them. The connections that make up the network are of two types: some are one-dimensional connections arising through the symmetry, while others are transversal intersections of two-dimensional invariant manifolds.

We combine techniques such as quotient by group actions, study of Poincaré maps and symbolic dynamics. We prove switching at each node of a two-node network: trajectories

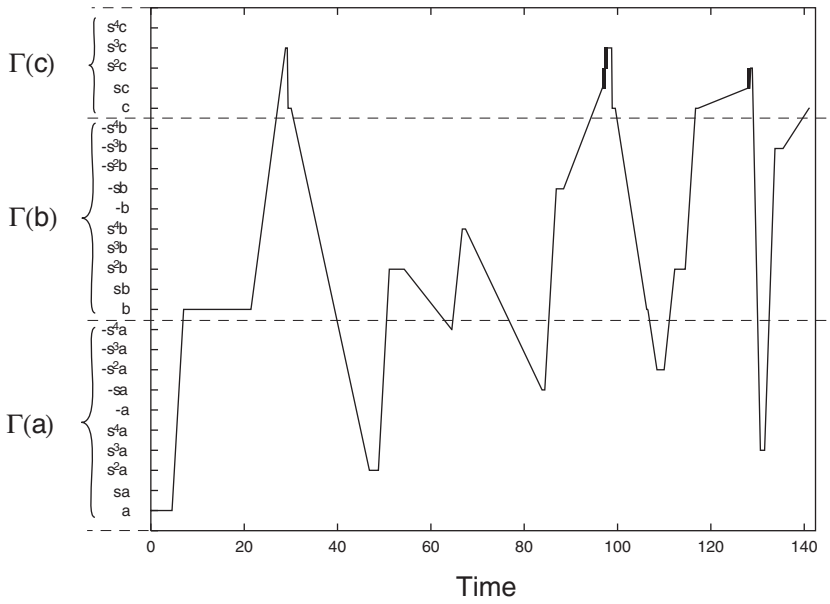

Figure 8. Sample output from running the C-routine for equations (1), for parameter values $\lambda = 1$, $\beta = 1$ and $\gamma = -0.6$, with initial conditions near equilibrium a, $(x_1, y_1, x_2, y_2) = (0.7907, 0.0001, 0.7904, -0.0001)$.

arriving near one of the nodes may follow along any of the connections departing from it. We also obtain switching on the network: every infinite path on the network is followed by a neighbouring trajectory. This is a new mechanism for switching, that arises from the transversal intersection of the invariant manifolds together with complex eigenvalues.

Bigger networks for vector fields with larger symmetry groups may reduce to the case discussed above through a quotient by part of the symmetry. We apply this method to an example and show how to lift the information on the dynamics to the larger network, to obtain both switching and a horseshoe of suspended horseshoes.

We end with the conjecture that if in the two-node network in section 6 only one of the saddles possessed complex eigenvalues, then switching and horseshoes would still be present.

Acknowledgments

The authors are grateful to Mike Field for very useful discussions and suggestions. These took place both in Houston and in Porto and benefitted from financial support from Fundação Luso-Americana para o Desenvolvimento and Fundação para a Ciência e a Tecnologia. Part of this work was done while the first author was on leave from the Faculdade de Economia do Porto and receiving a Prodep grant.

Appendix

We give a brief explanation of how the routine `field_aux()` we have added to our Dstool specification of Field's example works. We present a picture illustrating one sequence of output (see figure 8) showing evidence of some of the connections. The routine and the Dstool specification are available as supplementary data at stacks.iop.org/Non/18/391.

We create arrays containing the coordinates of the equilibria and their identification.

For each coordinate of the actual position in phase space, the routine `field_aux()` first computes its distance to the coordinates of an equilibrium. Then it compares each of those values with a pre-defined distance. This is repeated for each point in the array of equilibria. The pre-defined distance is considered as a parameter and so its value can be changed during the Dstool execution.

If the distance computed in each coordinate is less than the fixed distance, this means that the trajectory passes near the equilibrium that is being analysed. In this case it prints the identification of the equilibrium and the distance.

We study the proximity of a trajectory to a periodic trajectory by its proximity to some points of the periodic trajectory. We used Dstool to compute the coordinates in the (y_1, y_2)-plane of eight points that belong to the periodic trajectory c. The points of the remaining periodic trajectories are computed using the group action. All these points are stored in an array that is used to execute the procedure above.

References

[1] Aguiar M A D 2002 Vector fields with heteroclinic networks *PhD Thesis* Departamento de Matemática Aplicada Faculdade de Ciências da Universidade do Porto

[2] Aguiar M A D, Castro S B S D and Labouriau I S 2004 Simple vector fields with complex behaviour *Centro de Matemática da Universidade do Porto Preprint* CMUP 2004-24 http://www.fc.up.pt/cmup/

[3] Anosov D V (ed) 1995 *Dynamical Systems IX—Dynamical Systems with Hyperbolic Behaviour* (*Encyclopædia of Mathematical Sciences* vol 66) (Berlin: Springer)

[4] Armbruster D, Stone E and Kirk V 2003 Noisy heteroclinic networks *Chaos* **13** 71–9

[5] Ashwin P and Chossat P 1998 Attractors for robust heteroclinic cycles with continua of connections *J. Nonlinear Sci.* **8** 103–29

[6] Ashwin P and Field M 1999 Heteroclinic networks in coupled cell systems *Arch. Ration. Mech. Anal.* **148** 107–43

[7] Brannath W 1994 Heteroclinic networks on the tetrahedron *Nonlinearity* **7** 1367–84

[8] Campbell S A and Holmes P 1991 Bifurcation from O(2) symmetric heteroclinic cycles with three interacting modes *Nonlinearity* **4** 697–726

[9] Chawanya T 1997 Coexistence of infinitely many attractors in a simple flow *Physica* D **109** 201–41

[10] Chossat P, Guyard F and Lauterbach R 1999 Generalized heteroclinic cycles in spherically invariant systems and their perturbations *J. Nonlinear Sci.* **9** 479–524

[11] Dias A P S, Dionne B and Stewart I 2000 Heteroclinic cycles and wreath product symmetries *Dyn. Stab. Syst.* **15** 353–85

[12] Field M J 1980 Equivariant dynamical systems *Trans. Am. Math. Soc.* **259** 185–205

[13] Field M J 1989 Equivariant bifurcation theory and symmetry breaking *J. Dyn. Diff. Eqns* **1** 369–421

[14] Field M J and Richardson R W 1992 Symmetry-breaking and branching patterns in equivariant bifurcation theory, II *Arch. Ration. Mech. Anal.* **120** 147–90

[15] Field M and Swift J W 1992 Stationary bifurcation to limit cycles and heteroclinic cycles *Nonlinearity* **4** 1001–43

[16] Field M J 1996 *Lectures on Bifurcations, Dynamics and Symmetry* (*Pitman Research Notes in Mathematics Series* vol 356) (Harlow: Longman)

[17] Guckenheimer J and Holmes P 1983 *Nonlinear Oscillations, Dynamical Systems, and Bifurcations of Vector Fields* (*Appl. Mathematical Sci.* number 42) (New York: Springer)

[18] Guckenheimer J, Meloon B A, Myers M R, Wicklin F J and Worfolk P A 1997 *DsTool: A Dynamical System Toolkit with an Interactive Graphical Interface—User's Manual* Version Tk Draft Center for Applied Mathematics, Cornell University

[19] Guckenheimer J and Worfolk P 1992 Instant chaos *Nonlinearity* **5** 1211–22

[20] Junge O 2000 *GAIO—Reference Manual Version 1.2* Department of Mathematics and Computer Science, University of Paderborn

[21] Kirk V and Silber M 1994 A competition between heteroclinic cycles *Nonlinearity* **7** 1605–21

[22] Krupa M 1997 Robust heteroclinic cycles *J. Nonlinear Sci.* **7** 129–76

[23] Lauterbach R and Roberts M 1992 Heteroclinic cycles in dynamical systems with broken spherical symmetry *J. Diff. Eqns* **100** 22–48

[24] Melbourne I, Chossat P and Golubitsky M 1989 Heteroclinic cycles involving periodic solutions in mode interactions with O(2) symmetry *Proc. R. Soc. Edinb.* A **113** 315–45
[25] Reissner E 1999 *On Flows with Spatio-Temporal Symmetries near Heteroclinic Networks* (Aachen: Shaker) Augsburg University Dissertation
[26] Samovol V S 1972 Linearization of a system of differential equations in the neighborhood of a singular point *Sov. Math. Dokl.* **13** 1255–9
[27] Silber M, Riecke H and Kramer L 1992 Symmetry-breaking Hopf bifurcation in anisotropic systems *Physica* D **61** 260–78
[28] Wiggins S 1988 *Global Bifurcations and Chaos—Analytical Methods* (New York: Springer)
[29] Worfolk P A 1996 An equivariant, inclination-flip, heteroclinic bifurcation *Nonlinearity* **9** 631–47